Electric Power Systems Research 116 (2014) 94–105

Contents lists available at ScienceDirect

Electric Power Systems Research

journal homepage: www.elsevier.com/locate/epsr

Phasor-based assessment for harmonic sources in distribution networks

Reza Arghandeh[a,*], Ahmet Onen[b], Jaesung Jung[b], Danling Cheng[c], Robert P. Broadwater[b], Virgilio Centeno[b]

[a] California Institute for Energy and Environment (CIEE), Electrical Engineering and Computer Science (EECS), University of California, Berkeley, 2087 Addison Street, 2nd Floor, Berkeley, CA 94704-1103, USA
[b] Department of Electrical and Computer Engineering, Virginia Polytechnic Institute and State University, Blacksburg, VA, USA
[c] Electrical Distribution Design, Inc., Blacksburg, VA, USA

ARTICLE INFO

Article history:
Received 23 January 2014
Received in revised form 18 May 2014
Accepted 20 May 2014

Keywords:
Distribution network
Harmonics
Distortion
Power quality
Phase coupling
Phase balancing

ABSTRACT

Phasor-based interdependencies of multiple harmonic sources, especially Distributed Energy Resources, on distribution networks are analyzed in this paper. A new index, Phasor Harmonic Index (IPH), is proposed by the authors. IPH considers both harmonic source magnitude and phase angle for different harmonic orders. Other commonly used harmonic indices are based solely on magnitude of waveforms. A very detailed model of a distribution network is used in the harmonic assessment. With the help of the detailed distribution network model, the phase couplings and the phase balancing impacts on harmonic propagation between three phases are investigated. Moreover, effects of harmonic source phase angle deviations are analyzed at both the customer side and the substation side. This paper investigates the importance of phase angles in harmonic assessment and how distribution network characteristics can be analyzed appropriately with phasor-based harmonic studies. In addition to device level harmonics, system level harmonic propagation need to be considered.

1. Introduction

The resultant harmonics from Distributed Energy Resources (DER) inverters and the spread of power-based appliances create concerns for power system operators and engineers. Harmonic propagation causes distortion in voltage and current waveforms in different parts of distribution networks. Harmonics generated by different harmonic sources can interact to either increase or decrease the effects of harmonics.

The harmonic impact on power systems is a well-researched topic. Harmonic measurement and filtering in power systems are discussed in many literatures like [1,2]. However, existing researches mostly consider harmonics as a local phenomenon with local effects [3,4]. There are a few papers that focus on harmonics from Distributed Energy Resources (DER) [5–7]. Authors in [8,9] focus on harmonic filter design for DER units. However, the proposed solutions are local approaches for controlling each inverter. Even less literature investigates the impact of harmonic propagation in distribution networks. Authors in [10] proposed a method to find locations of major harmonic sources in distribution networks. The authors use the Norton equivalent model for the distribution network which is not a full representative of the network. [11] analyzes harmonic distortion in different types of distribution transformers. [12] conducts a sensitivity analysis to find vulnerable buses in distribution networks. But, the authors use the Thevenin equivalent model at each bus instead of the full topological model of the circuit. [13,14] shows the impact of aggregated harmonics from Distributed Generation units in distribution networks. However, they use a single-phase equivalent line model and do not consider multi-phase line models.

The novelty of this paper is in investigating the system-wide harmonic interaction between different harmonic sources, mainly DERs. In the literature there has been a lack of physical-based, detailed models in harmonic studies. The harmonic investigation in this paper benefits from a detailed distribution network model. The model employed has large numbers of single phase, multi-phase, and unbalanced loads. These details of distribution system modeling have not been addressed in previous harmonic analysis found in the literature.

This paper proposes a new index based on the harmonic source phase angle. In terms of harmonic distortion quantization, the Total Harmonic Distortion (THD) is the most common index in

* Corresponding author. Tel.: +1 949 943 5600.
E-mail address: arghandehr@gmail.com (R. Arghandeh).

http://dx.doi.org/10.1016/j.epsr.2014.05.012
0378-7796/

Nomenclature

V_h	voltage magnitude for frequency order h
I_h	current magnitude for frequency order h
V_{Total}	total value for voltage magnitude
I_{Total}	total value for current magnitude
V_h^{Ph}	phasor form of voltage for frequency order h
I_h^{Ph}	phasor form of current for frequency order h
θ_h	harmonic current phase angle
φ_h	harmonic voltage phase angle
h	harmonic frequency order
THDV	voltage total harmonic distortion
THDI	current total harmonic distortion
IPHV	voltage index of phasor harmonics
IPHI	current index of phasor harmonics
IHDI	individual harmonic index for current
IHDV	individual harmonic index for voltage
PTM	phase Thevenin equivalent matrix

the literature [15,16]. But, THD is based only on the magnitude of the distorted waveforms. In this paper a new index is proposed called the Index of Phasor Harmonics (IPH). IPH incorporates both magnitude and phase angle information in evaluating distorted waveforms resulting from the interaction of multiple harmonic sources. The advantages of IPH as compared to common harmonic indexes are illustrated in case studies.

This paper also analyzes the interactions of multiple harmonic sources in a three phase, asymmetrical and unbalanced distribution network. The way DER inverters can work together to either decrease or increase harmonic distortion throughout the distribution network is investigated.

The phase coupling impact on harmonic propagation has not been addressed in previous works, especially for distribution networks. Because of short distances between conductors in overhead lines and underground cables, phase coupling in distribution networks needs to be considered in harmonic analysis. In this paper, the IPH index is used to measures the impact of a harmonic sources attached to one phase on other phases.

There are a few papers that consider the impact of phase balance on harmonics [17–19]. However, they are all at the device level. That is, they focus on harmonic and load balancing in transformers and inverters. Another novelty of this paper is analyzing the impact of phase balance at the feeder level on harmonic distortion throughout the whole feeder.

The paper is organized as follows: Section 2 discusses harmonics analysis. Section 3 describes the impacts of source and network characteristics on harmonics. Section 4 presents conclusions and observations.

2. Harmonic analysis in distribution networks

2.1. Indices for measuring harmonic distortion

Harmonic components in AC power systems are sinusoidal waveforms that are integer multiples of the fundamental frequency. The summation of harmonic components results in distorted current and voltage waveforms. Periodic functions of distorted voltage and current are defined by Fourier series as follows

$$I_{\text{Total}} = \sum_{h=1}^{\infty} \sqrt{2} I_h \sin(h\omega_0 t - \theta_h) \tag{1}$$

$$V_{\text{Total}} = \sum_{h=1}^{\infty} \sqrt{2} V_h \sin(h\omega_0 t - \varphi_h) \tag{2}$$

where I_{Dist} and V_{Dist} are the distorted current and voltage at the measurement point, respectively. I_h and V_h are current and voltage r.m.s. values for the hth harmonic order. θ_h and φ_h are harmonic current and voltage phase angles. ω_0 is the fundamental angular frequency and h is the harmonic frequency order. n is number of harmonic orders considered.

The most common index used for measuring harmonics in standards and literature is Total Harmonic Distortion (THD) [16]. THD includes the contribution of the magnitude of each harmonic component as given by

$$\text{THDI} = \frac{1}{I_1}\sqrt{\sum_{h=2}^{\infty} I_h^2} \tag{3}$$

$$\text{THDV} = \frac{1}{V_1}\sqrt{\sum_{h=2}^{\infty} V_h^2} \tag{4}$$

where THDI and THDV are THD values for current and voltage, respectively. I_1 and V_1 are the current and voltage r.m.s. values for the fundamental frequency, respectively.

Another widely used index is Individual Harmonic Distortion (IHD). IHD represents the percentage of each harmonic order amplitude relative to the fundamental voltage or current, as given by

$$\text{IHDI} = \frac{I_h}{I_1} \times 100 \tag{5}$$

$$\text{IHDV} = \frac{V_h}{V_1} \times 100 \tag{6}$$

where IHDI and IHDV are the IHD index for voltage and current, respectively. The THD and IHD are addressed in IEEE-519, IEEE-1547, IEC-610000, and EN50160 and other standards for power quality and distribution network related products [20–22].

In some standards, the conventional definition of power factor is modified to account for the contribution of higher frequencies [16]. The modified power factor is called Total Power factor (TPF). Eq. (7) shows the relationship between TPF and THD [23]:

$$\text{TPF} = \frac{\cos\delta_1}{\sqrt{1+\text{THDI}^2}} \tag{7}$$

where δ_1 is the angle between voltage and current at the fundamental frequency, where $\cos(\delta_1)$ is called the displacement power factor and the factor $1/\sqrt{1+\text{THDI}^2}$ is called the distortion power factor.

The THD and IHD indices are only based on the magnitude of harmonic components. The TPF only considers the phase angle difference between the fundamental voltage and current vectors. Therefore, the most common indices for harmonic analysis do not account for the phase angles of the higher frequencies harmonic components in harmonic distortion assessment. However, the vectorial characteristics of the harmonic waveforms with higher frequencies do have an impact on the total distorted current or voltage waveforms.

In this paper a new harmonic assessment index, Index of Phasor Harmonic (IPH), is used. The IPH is proposed by authors. More mathematical insight into the index is presented in [24] by authors. The IPH considers information related to both magnitudes and phase angles of the harmonic components based on the waveform orthogonal decomposition. The purpose is to resolve voltage or current values along directions of in-phase component of the

nonsinusoidal waveform. Using the sine identity (1) and (2) can be rewritten in the orthogonal form as:

$$I_{\text{Total}} = \sqrt{2}\sum_{h=1}^{\infty} I_h \cos(\theta_h)\sin(h\omega_0 t) - \sqrt{2}\sum_{h=1}^{\infty} I_h \sin(\theta_h)\cos(h\omega_0 t) \quad (8)$$

$$V_{\text{Total}} = \sqrt{2}\sum_{h=1}^{\infty} V_h \cos(\varphi_h)\sin(h\omega_0 t) - \sqrt{2}\sum_{h=1}^{\infty} V_h \sin(\varphi_h)\cos(h\omega_0 t) \quad (9)$$

In (8) and (9), total current and voltage are separated into two in-phase and in-quadrature components. The IPH is obtained by dividing the summation of in-phase harmonic components by the algebraic sum of harmonic waveform magnitudes. The IPH equations are as follow:

$$\text{IPHI} = \frac{\sum_{h=1}^{\infty} |I_{hP}|}{\sum_{h=1}^{\infty} |I_h|} \quad (10)$$

$$\text{IPHV} = \frac{\sum_{h=1}^{\infty} |V_{hP}|}{\sum_{h=1}^{\infty} |V_h|} \quad (11)$$

where IPHI and IPHV are the Index of Phasor Harmonics for current and voltage waveforms, respectively. The I_{hP} and V_{hP} are in-phase components of current and voltage as follows:

$$I_{hP} = \sqrt{2} I_h \cos(\theta_h) \quad (12)$$

$$V_{hP} = \sqrt{2} V_h \cos(\varphi_h) \quad (13)$$

IPH indices are compared to THD indices in the following sections.

2.2. Integrated system modeling approach for harmonic analysis

The Integrated System Model (ISM) is intended to include all objects found in the field- every bus in the substation, every sectionalizing device (even switches in parallel), and every support structure (poles, manholes, towers, etc.). This way realistic scenarios can be supported and simulation results can be trusted.

The unique utility specific model referred to as the Integrated System Model (ISM) is developed in the DEW environment. The ISM is associated with a database for the geographical information (GIS), component parameters, transformers parameters, conductors sizing, and load and generation characteristics [25]. The ISM can model multi-phase, unbalanced, asymmetrical distribution networks. The ISM modeling approach is in opposition to the current industry practice of having different models and software packages for the same circuit. Moreover, the ISM offers a graph-based topology iterator framework that facilitates computations for power flow and other calculations on the large scale model [26]. The ISM uses an edge-edge graph model. The status of each network component is updated locally. Therefore, changes in topology are handled locally without large and sparse matrices. [26,27] provide further explanation about ISM modeling. The [28] presents more information about ISM load modeling and [29] is focused on the mathematical approaches for power flow analysis in ISM.

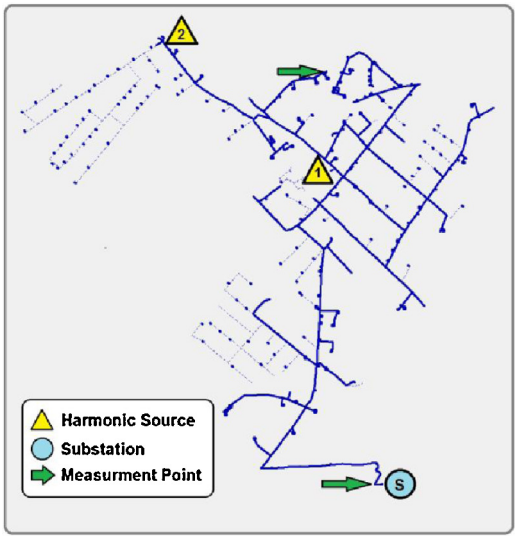

Fig. 1. Schematic of distribution network model used for studying interactions of multiple harmonic sources. Triangles indicate locations of harmonic sources and arrows indicate locations where harmonics are evaluated.

Phasor-based harmonic analysis presented in this paper takes advantage of the physical representation of the distribution network (topology) which is embedded in the ISM model. Fig. 1 depicts the ISM circuit model that is used as case study in this paper.

The ISM model used for the case study is an actual residential circuit in the state of New York with a 9.6 MVA annual peak load on a 13.2 kV distribution feeder [30]. It has single phase and multiphase unbalanced loads with 329 residential and commercial customers. In this case study, there are two harmonic sources indicated with triangular symbols. However, the algorithm described herein for phasor-based harmonic analysis is not limited by the number of DER units in a feeder. The harmonic calculations are presented at two points indicated by arrows in Fig. 1. The first point is the

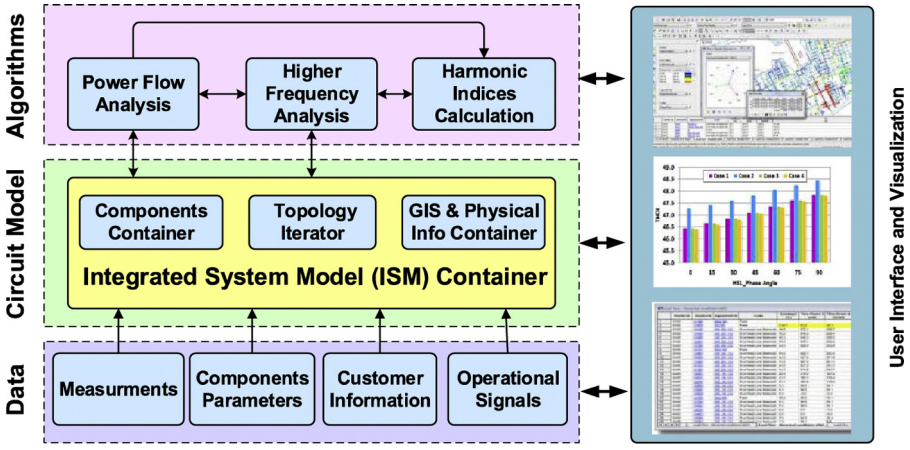

Fig. 2. Architecture of harmonic analysis.

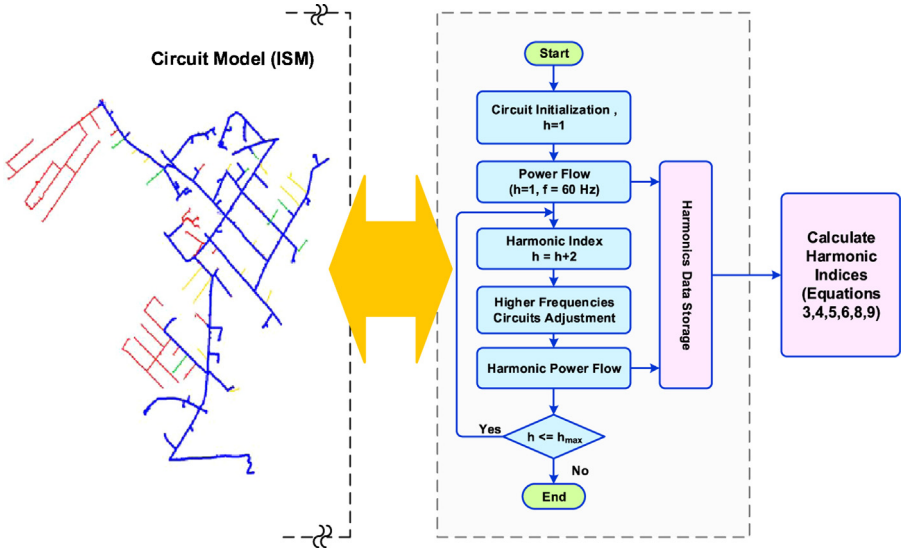

Fig. 3. Harmonic indices calculation diagram.

substation, and the second point is at the secondary of a distribution transformer located between the two harmonic sources.

The architecture for the phasor-based harmonic analysis is illustrated in Fig. 2. Phasor-based harmonic analysis has three layers, data, model and analytics. The data layer contains data interfaces for the distribution network model. The measurements, component parameters, customer information, and operational signals, like distribution network operator commands, are attached to the ISM model. The circuit model is ISM model that is explained. The phasor-based harmonic assessment algorithm starts with calculating voltage and current magnitude and phase angle on all nodes of the distribution circuit at fundamental frequency without harmonic sources (base case). Then, harmonic source are added to the ISM model. The harmonic sources can be a distributed energy resource, energy storage, load or any power electronic interface connected to the feeder (here referred to as DER).

Because circuit characteristics are subject to changes in higher frequencies, distribution network components like conductors, transformers and load impedances have to be modified to the analysis frequency level. In this paper actual harmonic measurement data are used. Information regarding harmonic source and circuit characteristics of higher harmonics will be presented in Section 3.1.

The other important issue in phasor-based harmonic assessment is related to harmonic distortion caused by the aggregation of different frequency components. To simulate and calculate the overall distortion, the algorithm has to store high frequency voltage and current components separately in a database to calculate harmonic assessment indices in Section 2.1.

The phasor-based harmonic assessment algorithm is composed of the following steps:

(1) Update DEW-ISM model with available measurements for generation and loads.
(2) Voltage and current magnitude and phase angle value calculations in the ISM model for fundamental frequency without harmonic sources (base case), where calculated results are stored to the database.
(3) The ISM model components modification for higher harmonics. ("*N*" is the maximum harmonic order for the analysis).
(4) Calculate voltage and current magnitudes and phase angle values for "*n*th" harmonic order, storing results in the database.
(5) if $n < N$, $n = n + 1$ and go to step 4, else go to step 6.
(6) Calculate THD, IPH indices (equations numbers).

In this paper *N* is 11. Fig. 3 illustrates the diagram for the phasor-based harmonic analytic section.

3. Impacts of source and network characteristics on harmonics

Harmonic propagation in distribution networks depends on a number of factors related to harmonic sources and distribution network characteristics. In this section the impact of harmonic source phase angle on harmonic propagation with multiple sources is addressed. Moreover, impacts of conductor phase coupling and load balance on harmonic propagation are investigated.

In this paper the main objective is investigating the importance of phase angles in harmonic assessment and how distribution network characteristics can be analyzed appropriately with a phasor-based harmonic analysis approach. The IPH index is applied and is compared to the conventional THD index. This paper focuses on analyzing the change in THD and IPH via phase angle variation.

3.1. Salient features of simulations

The research objective is the harmonic impact study apart from the harmonic source technology. There are two 3-phase harmonic sources in the distribution network. All phases of the harmonic sources have the same magnitudes. The harmonic magnitudes are based on actual measurement data from field tests on a DER inverter as shown in Fig. 4.

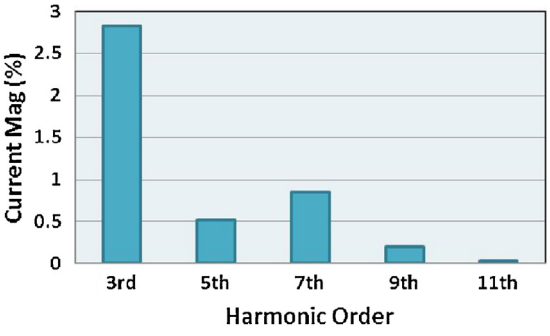

Fig. 4. Harmonic source magnitudes from field measurement data.

Table 1
Three phase harmonic angle sequences.

Order	Frequency	Sequence
0	60	+
3	180	0
5	300	–
7	420	+
9	540	0
11	660	–

The dominant current and voltage harmonic observed through the simulation are of the 3rd, 5th, 7th, 9th and 11th orders. Harmonics of higher orders are neglected due to their small values. In this case study, circuit analysis shows resonance frequency is much higher than the 11th harmonic order (660 Hz), so it does not impact the simulation results.

The phase rotation sequences of the harmonic source phase angles are presented in Table 1, where positive, zero, and negative sequence rotations are indicated with +, 0, and –, respectively. In simulations, the phase angle values for harmonics sources are shifted in addition to these sequential rotation between different harmonic orders.

To assure simulation results are not affected with resonance, several different scenarios with different magnitude phase angles are simulated. Part of the scenarios are reported in [24]. The objective of this paper is phasor-based interactions between different harmonic sources. So, the focus of the simulations presented here is on phase angle variations.

3.2. Source capacity and harmonic emission

To show the impacts of DER source capacity on the harmonic distortion at the substation, the simulation is conducted for two DERs, at the HS1 and HS2 points shown in Fig. 1 (the HS means harmonic source on the circuit schematic). It is assumed that the two DER sources inject power into the circuit with different percentages of their nominal capacity (3.8 kW). Phase angles have the same sequence as Table 1. Fig. 5 shows the variation of phase A THDI at the substation as a function of variation of the DERs capacity.

The THDI values increase with increasing harmonic source amplitudes, as expected. The next section is focused on the harmonic source phase angle relationship with harmonic interactions within the circuit.

3.3. Impact of harmonic source phase angle

In systems with multiple harmonic sources, the harmonic distortion interactions are impacted by the vectorial characteristics of the injected harmonic currents. The impact of each harmonic source's phase angle is investigated in this section. For sensitivity analysis purposes, harmonic source phase angles with frequency

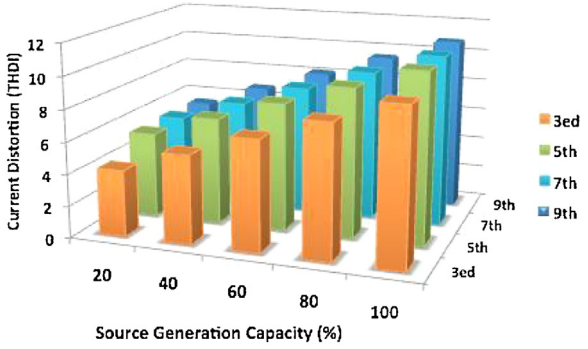

Fig. 5. DER Capacity vs. THDI at the substation.

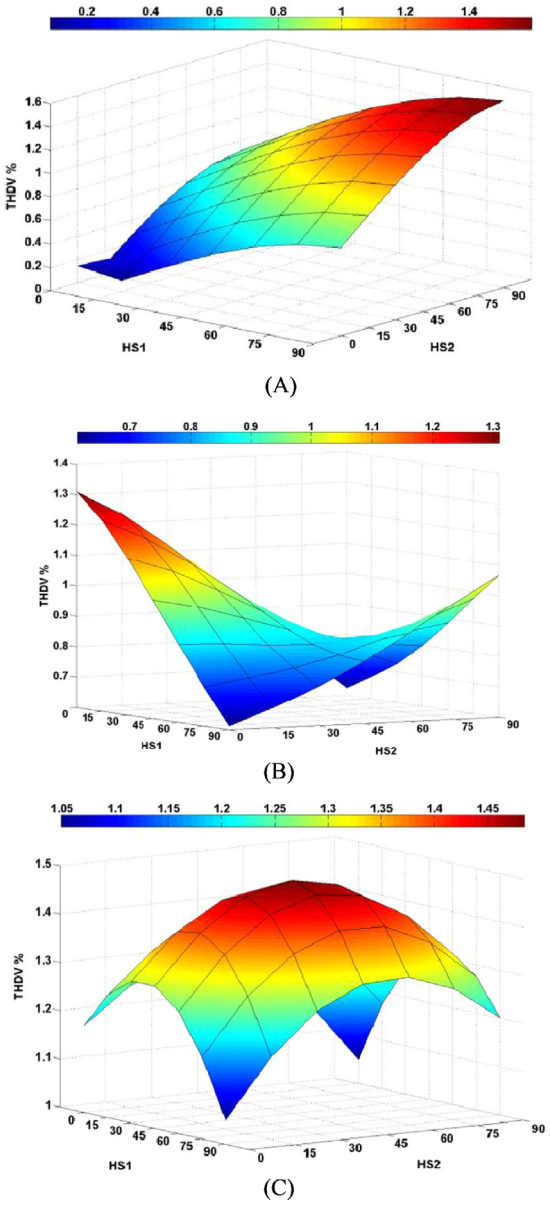

Fig. 6. THDV for phases A (A), B (B), and C (C) as a function of harmonic source 1 (HS1) and harmonic source 2 (HS2) phase angles.

shifts as (0°, 15°, 30°, 45°, 60°, 75°, 90°) from the reference phase angle are considered (see Table 1). For simulation purpose, all harmonic frequencies assumed to have same phase angle shift. When varying the phase angles of the harmonic sources, the magnitudes of both harmonic sources are maintained as given in Figs. 6 and 7. Fig. 6 shows THDV for different phase angle values at the substation point for each of the three phases.

As illustrated in Fig. 6, there are significant differences between THDV for the different phases. One reason for the variation of THDV is the different phase loading as presented in Table 2. Three phases mutual coupling is another reason for the difference in

Table 2
Unbalanced circuit loading at substation.

	Ph. A	Ph. B	Ph. C
Connected load (kW)	818.25	429.58	476.29
Connected load (kVar)	468.53	254.45	273.17
Current flow (Amps)	126.86	67.31	73.29

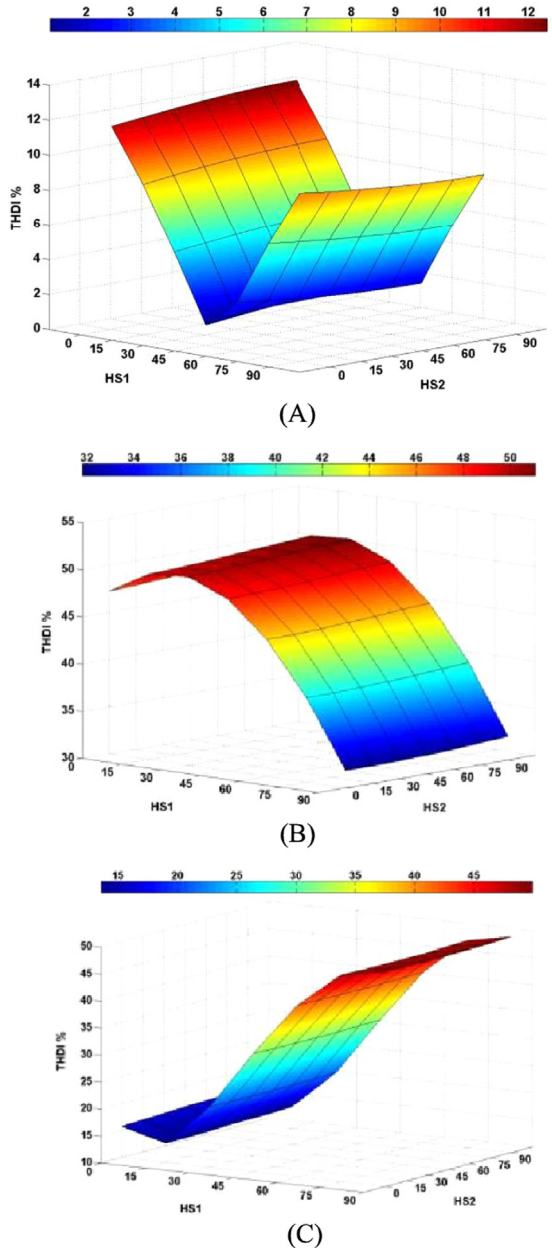

Fig. 7. THDI for phases A (A), B (B), and C (C) as a function of harmonic source 1 (HS1) and harmonic source 2 (HS2) phase angle.

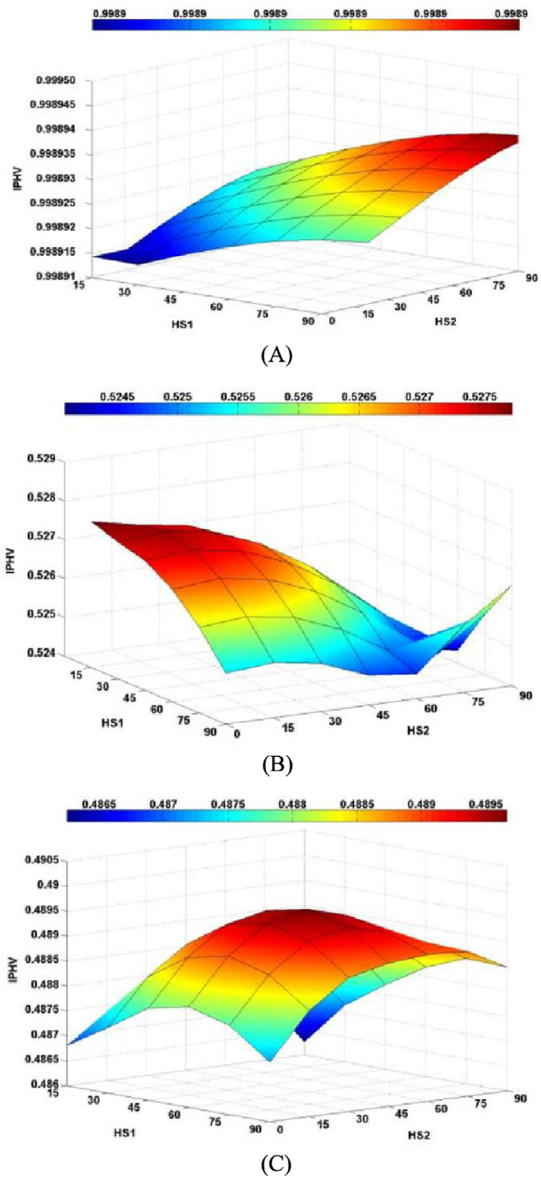

Fig. 8. IPHV values for harmonic sources 1 and 2 for different phase angles: phases A (A), B (B), and C (C).

the harmonic current propagations. The conductors coupling and phase balance are investigated more deeply in next sections.

The THDV surface plots in Fig. 6 are similar to hyperbolic geometrical functions. Fig. 6A shows THDV for phase A with a semi-spherical cliff with the minimum values at zero phase angle for both sources. The maximum values are achieved with 90° phase angle for both sources (THDV = 1.596). For Phase B, Fig. 6B, the saddle-shaped surface has the saddle point at 45° phase angle in both sources (THDV = 0.873), and the maximum THDV values occur at 0° and 90° for both sources. Phase C has a hemispherical plane with its maximum at 45° phase angle for both sources (THDV = 1.484). Observations show that the phase angles of the two harmonic sources affect the minimum and maximum THDV points at the substation.

The THDI surfaces in Fig. 7 shows that the first harmonic source has a larger impact on the harmonic current distortion at the substation. This observation reflects that the first harmonic source is closer to the substation than the second harmonic source. In Fig. 7A, the maximum THDI occurs at 0° for the first harmonic source and 90° for the second harmonic source. There is a canyon on the THDI surface for points with minimum THDI values at 45° for the first harmonic source. Finding points with minimum harmonic current distortion is important for harmonic control. At these points, the harmonic source contributions cancel each other out and cause the minimum current harmonic distortion.

The THDV and THDI sensitivity analysis shows that the extreme points occur around 0°, 45°, and 90° phase angles. The THDI and THDV minimum and maximum points are different, as are shown in Figs. 6 and 7. Relying on THDI and THDV brings more complexity to harmonic control in terms of focusing on voltage or current distortion. THDI and THDV are only based on harmonic source magnitudes. The IPHV index (Eq. (9)) results are presented in Fig. 8.

The proposed index in this paper, the IPH, includes phase angle values to present a more precise status of harmonic distortion in both the voltage and current waveforms. The IPHV geometrical variations for all phases show more correlation with the THDV surfaces in Fig. 6 and THDI surfaces in Fig. 7. However, the maximum

IPHV area for each phase is shifted slightly from the high THDV area to the high THDI area. Because the IPHV incorporates phase angle information, it is based on more information than THDV or THDI and this is reflected in the figures.

Refer to Fig. 7, parts B and C, where THDI values are high in comparison to THDV. This illustrates how phase angle changes can impact current distortion. However, the main aim is to show variations of THDV and THDI via phase angle changes. To have a more reliable and clear picture of harmonic emission in term of voltage and current, the new proposed index, IPHV is calculated for difference phase angles. The IPHV observation for phase A, Fig. 8A, shows more distortion around 90° phase angle for both harmonic sources. In phase B, Fig. 8B, the higher distortion area is extended to 0°–45° for both harmonic sources. The IPHV for Phase C, Fig. 8C, shows high distortion near 90° for both harmonic sources, as is in the THDI.

The simulation results, show the effectiveness of IPH in compare to the THD. The IPHV trend is similar to the voltage distortion. In this paper, the results are only presented for IPHV due to lack of space. The IPHI values present similar information. However, the IPHI trend is similar to the THDI.

3.4. Impact of conductors phase coupling

The harmonic behavioral difference between voltage and current in distribution networks is mostly caused by conductor impedances. Distribution network multi-phase structures, connection types, unbalanced loading and the greater variety of equipment in some ways makes for more complexity than found in transmission networks. The Thevenin equivalent impedance, as seen by harmonic sources, is applied in this section for sensitivity analysis purposes. It shows the importance of phase coupling impedances in overall distribution network modeling.

The Phase Thevenin Matrix (PTM) is a 3×3 matrix. It is derived by numerical approaches presented in [31]. To achieve the PTM, a test load is attached between phase and ground in grounded nodes and between two phases in ungrounded nodes. For each test load attachment, power flow is calculated to obtain voltage and current changes caused by the coupling between the phases and the connection point phase. The PTM is

$$\begin{bmatrix} V_{an} \\ V_{bn} \\ V_{cn} \end{bmatrix} = \begin{bmatrix} Z_{aa} & Z_{ab} & Z_{ac} \\ Z_{ba} & Z_{bb} & Z_{bc} \\ Z_{ca} & Z_{cb} & Z_{cc} \end{bmatrix} \times \begin{bmatrix} I_{an} \\ I_{bn} \\ I_{cn} \end{bmatrix} \tag{14}$$

$$\bar{\boldsymbol{V}} = \mathrm{PTM}_n \times \bar{\boldsymbol{I}} \tag{15}$$

where the diagonal elements represent, z_{ii}, self-impedance of each phase and off-diagonal elements, z_{ij}, represent coupling between phases i and j. Eq. (15) is the matrix form of (14). The PTM_n is the calculated Thevenin impedance at node n. $\boldsymbol{I}$ and $\boldsymbol{V}$ are the three phase current and voltage vectors. The Thevenin impedance matrixes in this section are in the form of ABC impedances. The PTM impedance seen by harmonic sources are as follows:

$$\mathrm{PTM}_{\mathrm{HS}_1} = \begin{bmatrix} 1.5111 + j\omega h \times 0.01269 & 0.1528 + j\omega h \times 0.00164 & 0.1519 + j\omega h \times 0.00136 \\ 0.1528 + j\omega h \times 0.00164 & 1.5095 + j\omega h \times 0.01262 & 0.1536 + j\omega h \times 0.00163 \\ 0.1519 + j\omega h \times 0.00136 & 0.1536 + j\omega h \times 0.00163 & 1.5089 + j\omega h \times 0.01266 \end{bmatrix} \tag{16}$$

$$\mathrm{PTM}_{\mathrm{HS2}} = \begin{bmatrix} 1.7328 + j\omega h \times 0.01458 & 0.2391 + j\omega h \times 0.00244 & 0.2376 + j\omega h \times 0.00202 \\ 0.2391 + j\omega h \times 0.00244 & 1.7325 + j\omega h \times 0.01449 & 0.2399 + j\omega h \times 0.00241 \\ 0.2376 + j\omega h \times 0.00202 & 0.2399 + j\omega h \times 0.00241 & 1.7304 + j\omega h \times 0.01454 \end{bmatrix} \tag{17}$$

As illustrated in Fig. 1, the second harmonic source is farther from the substation. Fig. 9 shows a schematic of the system equivalent PTM. The PTM depends on network topology and three phase coupling. To analyze the impacts of three phase network impedance on harmonic propagation, the PTM is calculated for four cases. The first case neglects the admittance terms in conductor lines. Generally the shunt admittance of overhead lines is small and can be neglected [32].

The second case neglects mutual coupling elements in the PTM. The PTM is diagonal in this case. The PTM impedance calculation in this case reduces the impact of topology on the harmonic propagation. The third case considers balanced impedance values for the three phases. The last case calculates the PTM without the previously mentioned simplifications. Table 3 shows the PTM impedance as seen by the first harmonic source for the four cases in the fundamental frequency.

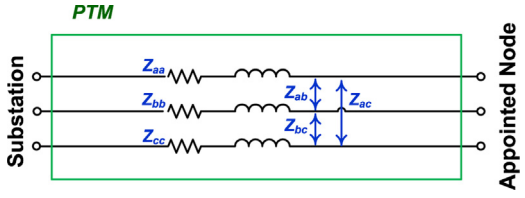

Fig. 9. Three-phase system PTM equivalent.

Table 3
PTM values for different cases.

Case	Description	PTM for HS1
1	Neglect shunt admittance	$\begin{bmatrix} 1.5102 + 4.7827j & 0.1528 + 0.6196j & 0.1518 + 0.5121j \\ 0.1528 + 0.6196j & 1.5090 + 4.7566j & 0.1537 + 0.6148j \\ 0.1518 + 0.5121j & 0.1537 + 0.6148j & 1.5084 + 4.7707j \end{bmatrix}$
2	Neglect mutual coupling	$\begin{bmatrix} 1.5111 + 4.7840j & 0 & 0 \\ 0 & 1.5094 + 4.7574j & 0 \\ 0 & 0 & 1.5094 + 4.7574j \end{bmatrix}$
3	Force balanced impedances	$\begin{bmatrix} 1.5132 + 4.7629j & 0.1529 + 0.5822j & 0.1531 + 0.5821j \\ 0.1529 + 0.5822j & 1.5075 + 4.7722j & 0.1525 + 0.5823j \\ 0.1531 + 0.5821j & 0.1525 + 0.5823j & 1.5089 + 4.7713j \end{bmatrix}$
4	Complete model values	$\begin{bmatrix} 1.7328 + 5.4966j & 0.2391 + 0.9180j & 0.2376 + 0.7603j \\ 0.2391 + 0.9180j & 1.7325 + 5.4627j & 0.2399 + 0.9097j \\ 0.2376 + 0.7603j & 0.2399 + 0.9097j & 1.7304 + 5.4831j \end{bmatrix}$

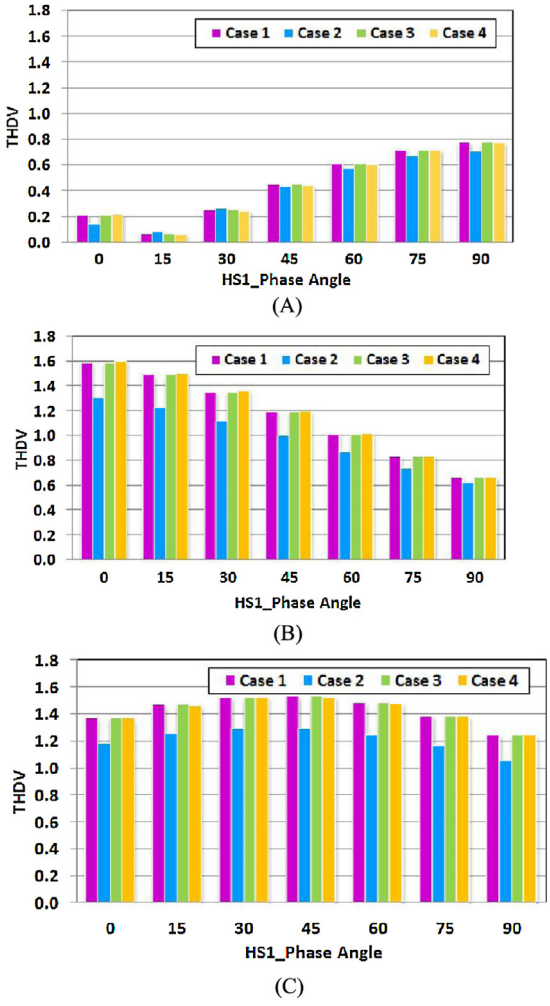

Fig. 10. THDV for phases A (A), B (B), and C (C) for different Thevenin impedance calculation cases.

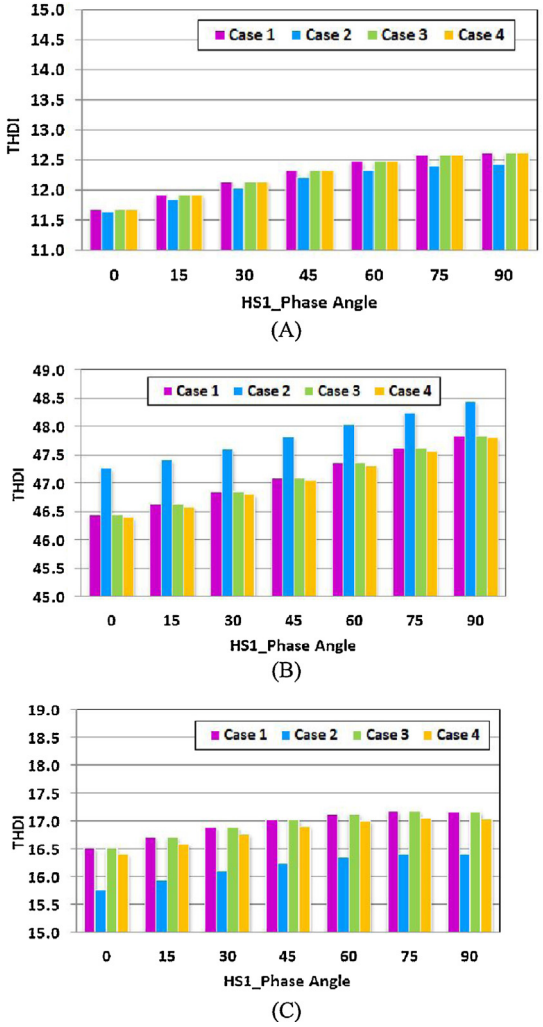

Fig. 11. THDI for phases A (A), B (B), and C (C) for different Thevenin impedance calculation cases.

Fig. 10 shows the THDV for the four cases of Table 3 at the substation. The phase angle for harmonic source 1 varies from 0° to 90° and phase angle for the second harmonic source is maintained at 0°. Fig. 10 shows that case 2, that ignores mutual coupling, has less voltage distortion than the other cases. Cases 1 and 3 have very close THDV results. However, case 4, the complete model, has slightly less THDV values than cases 1 and 3.

Fig. 11 shows the THDI for cases presented in Table 3. For THDI values, case 2 has the highest THDI. Similar to the THDV values, cases 1 and 3 have very close THDI values. However, case 4 is less than cases 1 and 3. The presented THDV and THDI values show that for this circuit ignoring admittance to simplify the PTM calculation does not make a big change in THDI and THDV values.

Moreover, forcing balanced values for the three phases impedance matrix as in case 3 does not make a big change, because harmonic source 1 is connected to the three phase line and the three phase conductors from the harmonic source to the substation have similar specifications in terms of length and conductivity. But case 2 shows that the phase coupling values cannot be ignored due to the considerable differences from the original case (case 4) in THDV and THDI achieved in the case 2 simulations.

The THDV and THDI differences are similar to the previous section, illustrating how phase angle variations can cause changes in current and voltage distortions. The work in this section presents harmonic distortion values under different assumptions for conductor impedance (or conductor model).

3.5. *Single phase harmonic sources and mutual coupling effects*

The phase coupling impact on harmonic propagation is not addressed in previous works, especially for distribution networks. Because of the short distance between overhead lines and underground cables in distribution networks, phase coupling in distribution conductors needs to be consider in harmonic analysis at the distribution level.

In this section, harmonic sources attached to one phase are analyzed to determine the impact on other phases. The single phase harmonic sources are located at the same place as the three phase harmonic sources (see Fig. 1). THDV and THDI are calculated at the substation. With harmonic current injections in only one phase, THDV and THDI indices for the other phases than the phase with the harmonic source are almost zero. However, mutual couplings do cause distortion in coupled voltage and current waveforms, but these are not reflected in the THDV and THDI indices. The IPHI index does provide non-zero harmonic distortion values for coupled phases. Fig. 12 depicts the statistical comparison of IPHI at the substation for the three phase harmonic source and the harmonic source considered in each phase separately. In Fig. 12, the IPHI values for different phase angles (0°–90°) of both harmonic sources are classified as a data set presented in the form of a Box Plot. The Box Plots show minimum, maximum, mean, and median values of IPHI calculated over the different phase angles.

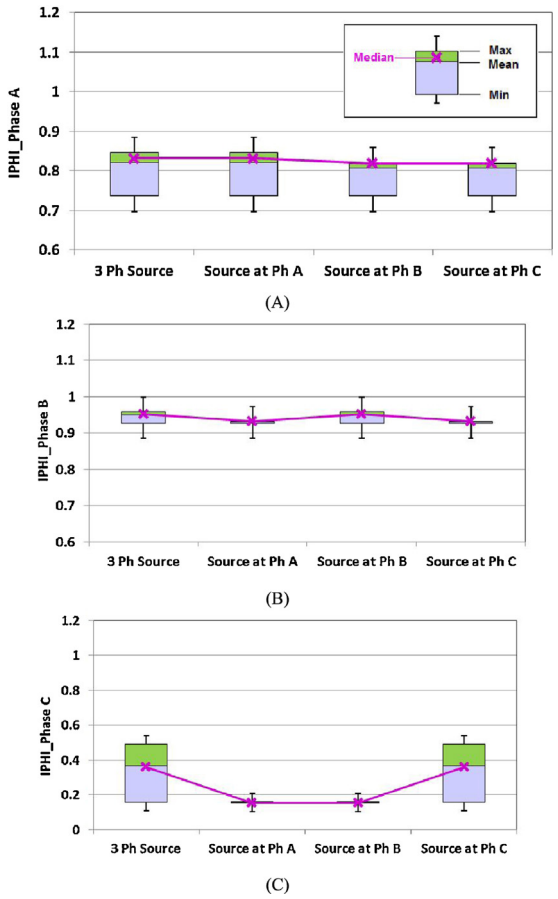

Fig. 12. BoxPolt for IPHI values with different harmonic source phase angles. (A) is for the harmonic source injections in only phase A, (B) is for the harmonic source injections in only phase B, and (C) is for the harmonic source injections in only phase C.

In Fig. 12A, IPHI is measured in phase A. For cases of three phase harmonic sources and phase A harmonic sources, the IPHI values are very similar. IPHI values for phase B and phase C are less than phase A, however they are not zero. In Figs. 11B and C there is a similar situation for phases B and C, respectively. The greater distance between the minimum and maximum values of IPHI in phase C shows that phase C has more sensitivity than the other phases to the harmonic source phase angle variations.

These types of sensitivity analyses are not possible with THDV and THDI indices because of the extremely small values of THD in the coupled phases that do not contain the harmonic source.

3.6. *Phase balance and harmonic propagation*

Phase balance affects harmonic propagation due to the change in power flow and the interphase couplings [33]. Phase balancing results in neutral current reduction and a decline in third harmonic currents [34]. In this paper, the phase balancing approach from [33] is applied. It is worth mentioning that phase balancing via phase moves is part of utility routine practice.

In this section the impact of phase balancing on harmonic distortion is analyzed with the help of THDV, THDI and IPHV indices. Fig. 13 shows the substation loading before and after phase balancing.

The phase balancing in this study includes re-phasing single-phase or double-phase laterals in the case study circuit model. After performing phase balancing, part of phase A lateral branches moved to phases B and C. There are totally 9 phase moves to balance the circuit.

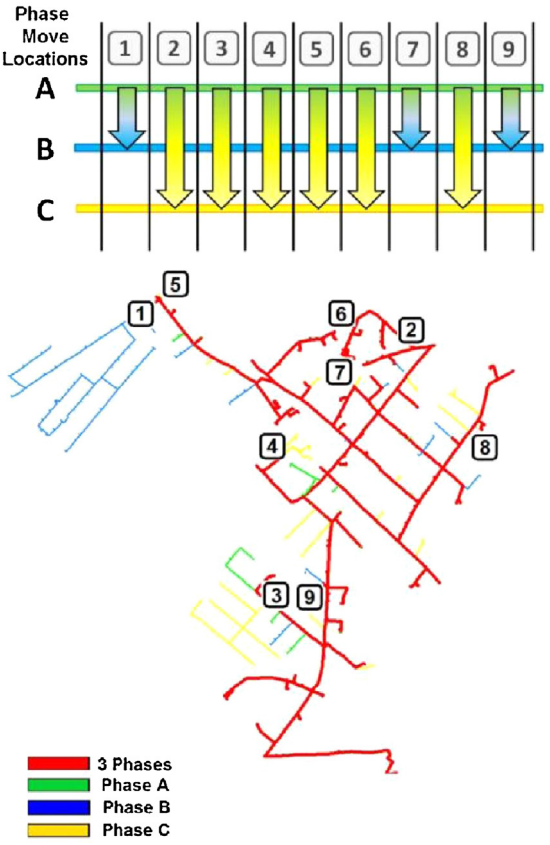

Fig. 13. Phase movements for circuit balancing. (For interpretation of the references to color near the citation of this figure, the reader is referred to the web version of the article.)

Fig. 13 depicts phase moves and their location in the distribution network. Phases are indicated in the figure with different colors. Locations in the circuit where phase moves occurred are numbered, and the associated graphic indicates the phase move that occurred at each numbered location. The arrows represent phase movements in different branches of the circuit. The arrows are colored based on phase changes (phase A → green, phase B → blue, phase C → yellow).

The substation THDV comparison for the balanced and unbalanced circuits are presented in Fig. 14. The THDV shows a small decrease for the balanced circuit. The THDI calculations are presented in Fig. 15. There is a decline in THDI for phases B and C, but phase A has an increase in THDI. However, the maximum THDI for the unbalanced case is 16.79 in phase B, and for the balanced case the maximum THDI is 13.42 in phase A. Thus, the maximum THDI over all of the phases decreased from the unbalanced case to the balanced case.

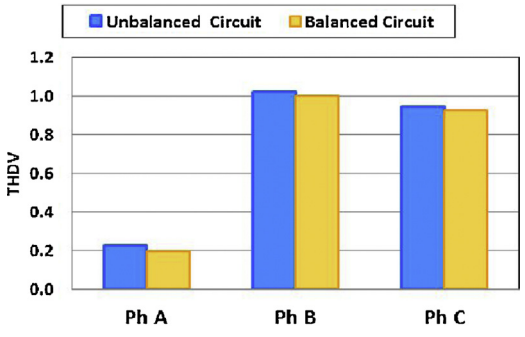

Fig. 14. THDV for balanced and unbalanced circuit.

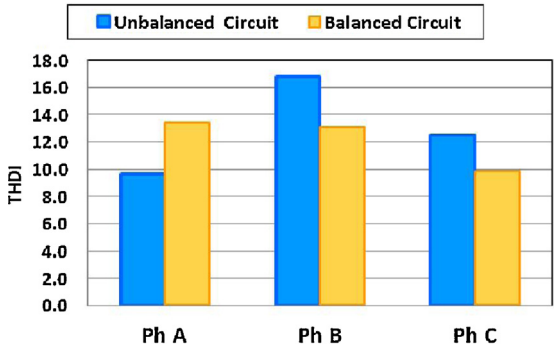

Fig. 15. THDI for balanced and unbalanced circuits.

Table 4
IPHV calculations for balanced and unbalanced cases.

IPHV	Ph. A	Ph. B	Ph. C
Balanced circuit	0.99990	0.51432	0.50107
Unbalanced circuit	0.99994	0.51608	0.49953
ΔIPHV (Bal – UnBal)	−0.00004	−0.00176	+0.00154
Σ (ΔIPHV) = −0.00026			

As illustrated in Figs. 13 and 14, THDV and THDI have different trends in phase balancing. The visual observation of THDI could create doubts about the positive impact of phase balancing on harmonic distortion.

Table 4 presents the IPHV calculation for the balanced and unbalanced circuit. Table 4 shows that the change in IPHV from the balanced case to the unbalanced case for Phase A and phase B have a negative IPHV, and phase C has a positive IPHV. The sum of the changes in IPHV shows a net decrease in harmonic distortion. Such a calculation cannot be performed with THDV and THDI.

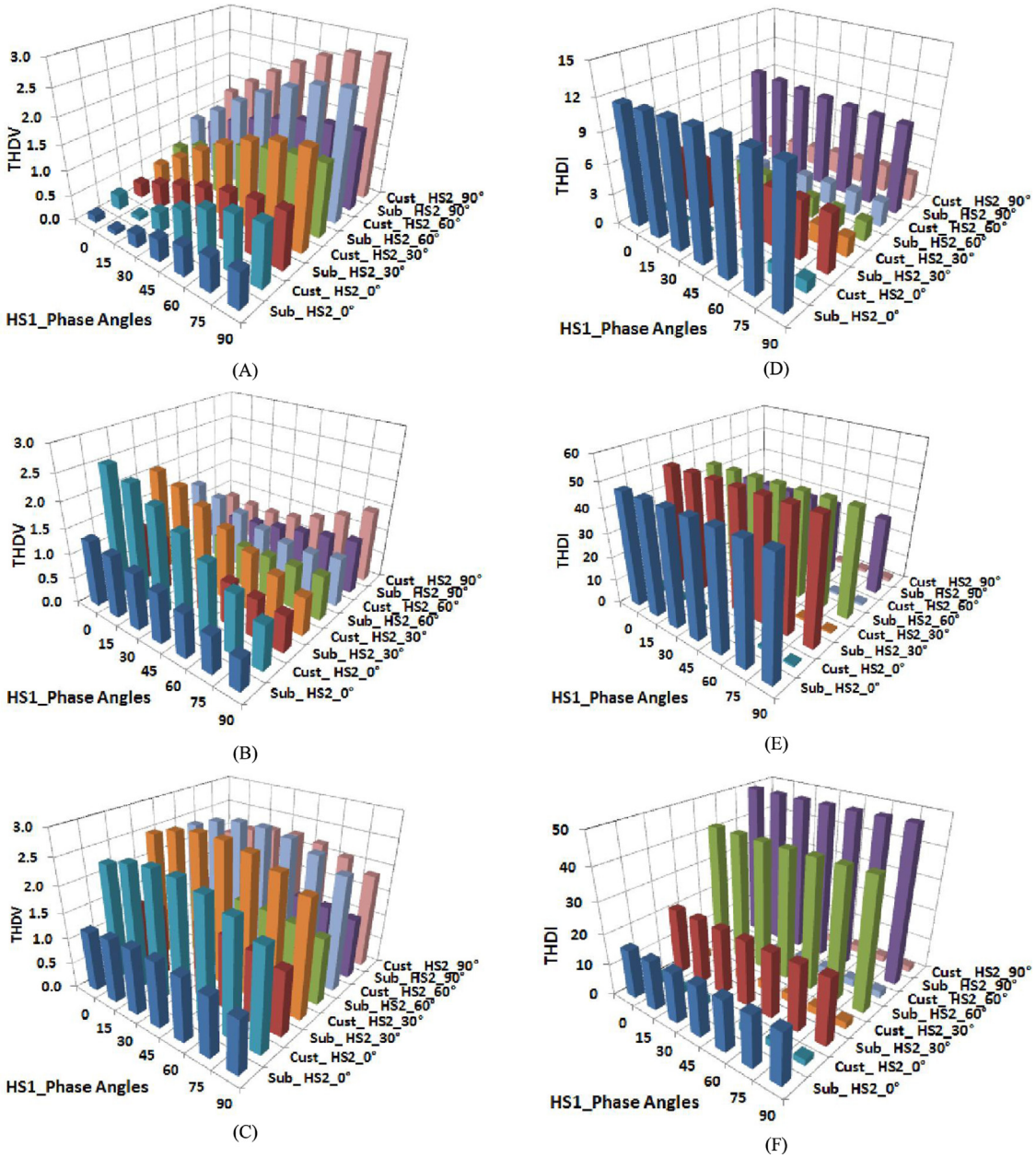

Fig. 16. THDV (A–C) and THDI (D–F) at the substation and a customer load point for each of the phases.

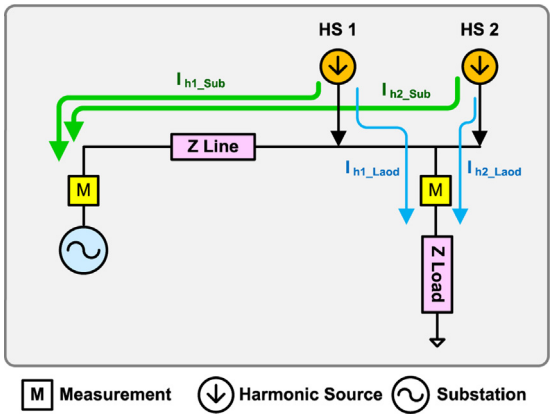

Fig. 17. Harmonic current distribution between load and substation.

3.7. Harmonic distortion levels at customer side vs. substation side

To demonstrate the harmonic distortion at different locations of the circuit, harmonic calculations are conducted at a customer load (secondary of distribution transformer) in this section. The measurement point is illustrated in Fig. 1. The customer side measurement point is between the harmonic sources. Fig. 16A–C shows THDV values at the substation and at the customer load. The HS1 means harmonic source 1. The "Sub_HS2_x°" means harmonic measurement at substation and harmonic source 2 has x° phase angle. The "Cust_HS2_x°" has similar meaning for measurement at customer side.

Fig. 16D–F presents the THDI values at the substation and at the customer load. It shows the substation experiences more distortion in current than the customer load. However, the customer load is exposed to higher harmonic voltage distortion. To explain these results, Fig. 17 depicts the equivalent circuit with measurement points and harmonic sources.

Since the impedance looking back into the substation is much smaller than the customer load impedance, a higher portion of harmonic currents flow to the substation than to the customer site. Therefore, the substation has more THDI. In this case study, the voltage distortion is larger at the customer load. Voltage is the product of impedance and current. The customer load impedance is much larger than the impedance of the path to the substation. The current through the load side is less, but the product of current and impedance for the customer side is higher than for the substation side. Therefore, more voltage distortion is realized at the customer side. This observation is illustrated in Fig. 17.

It is worth mentioning that when considering available standards for distribution network harmonics, the THDV and THDI at customer locations are within allowable ranges. However, the THDV and THDI at the substation exceeds the allowable ranges.

4. Conclusions and observations

This paper investigates the importance of phase angles in harmonic assessment and how distribution network characteristics can be analyzed with phasor-based harmonic studies. A detailed model of the distribution network is employed in the analysis. Several simulations and sensitivity analyses are presented that consider commonly used harmonic indices and a new proposed index, Index of Phase Harmonics (IPH), which takes into account information concerning phase angle differences. Conclusions and observations from the investigation here include:

(1) Understanding how multiple harmonic sources interact to increase or decrease the harmonic distortion is crucial in distribution networks and microgrids with large numbers of Distributed Energy Resources and harmonic problems. (2) The new proposed index, IPH, incorporates more information than the commonly used THDV and THDI indices, and IPH also provides more information in sensitivity analysis conducted in this paper. IPH considers the phase angles of the distorted voltage and current waveforms in the harmonic quantization, where the phase angle plays a significant role in the interactions of the harmonic sources. (3) Phase angles of harmonic sources have complex impacts on the overall harmonic distortion due to the vectorial summation of the injected harmonic currents. In some cases, phase angle variations of different harmonic sources result in reduced harmonic impacts. However, phase angle variations that increase harmonic distortion need to be understood. (4) The detailed circuit model employed and the IPH index pave the ground for the phase coupling sensitivity analysis performed. The simulation of multiphase modeling and unbalanced loads provides for more realistic harmonic propagation analysis. (5) The impact of phase balance on harmonic propagation in the distribution network is analyzed via a number of simulations. The results demonstrate that phase balancing can have a positive impact on harmonic reduction in distribution networks. (6) In quantizing the impact of single phase harmonic sources on other phases than its own phase, THDV and THDI values are very small. But, the equivalent Thevenin impedance analysis shows that the mutual coupling creates harmonic propagation in all phases. The proposed IPHI index is helpful in quantizing harmonic distortion in all phases with single phase harmonic sources present. (7) Harmonic impacts on customer loads and at the substation are evaluated. THD observations shows more current distortion at the substation than at the customer load. However, more harmonic voltage distortion is experienced at the customer load.

In harmonic studies and in harmonic measurements, harmonic distortion should be calculated throughout the distribution network considering harmonic source phase angle values. In addition to device level harmonics, system level harmonic propagation need to be considered.

References

[1] Kang F-s, S.-J. Park, S.E. Cho, J.-M. Kim, Photovoltaic power interface circuit incorporated with a buck-boost converter and a full-bridge inverter, Appl. Energy 82 (2005) 266–283.
[2] A. Marzoughi, H. Imaneini, A. Moeini, An optimal selective harmonic mitigation technique for high power converters, Int. J. Electr. Power Energy Syst. 49 (2013) 34–39.
[3] R.N. Ray, D. Chatterjee, S.K. Goswami, Reduction of voltage harmonics using optimisation-based combined approach, Power Electron. IET 3 (2010) 334–344.
[4] D. Salles, J. Chen, W. Xu, W. Freitas, H.E. Mazin, Assessing the collective harmonic impact of modern residential Loads— Part I: Methodology, IEEE Trans. Power Deliv. 27 (2012) 1937–1946.
[5] M. Farhoodnea, A. Mohamed, H. Shareef, A new method for determining multiple harmonic source locations in a power distribution system. Power and energy (PECon), in: 2010 IEEE International Conference, 2010, pp. 146–150.
[6] I.T. Papaioannou, A.S. Bouhouras, A.G. Marinopoulos, M.C. Alexiadis, C.S. Demoulias, D.P. Labridis, Harmonic impact of small photovoltaic systems connected to the LV distribution network. Electricity Market, in: 2008 EEM 2008 5th International Conference on European, 2008, pp. 1–6.
[7] H.E. Mazin, X. Wilsun, H. Biao, Determining the harmonic impacts of multiple harmonic-producing loads, IEEE Trans. Power Deliv. 26 (2011) 1187–1195.
[8] X. Wang, F. Blaabjerg, Z. Chen, Synthesis of variable harmonic impedance in inverter-interfaced distributed generation unit for harmonic damping throughout a distribution network, IEEE Trans. Ind. Appl. 48 (2012) 1407–1417.
[9] P. HESKES, J. DUARTE, Harmonic reduction as ancillary service by inverters for distributed energy resources (DER) in electricity distribution networks, in: Proc CIRED, 2007, pp. 1–4.
[10] M. Farhoodnea, A. Mohamed, H. Shareef, H. Zayandehroodi, An enhanced method for contribution assessment of utility and customer harmonic distortions in radial and weakly meshed distribution systems, Int. J. Electr. Power Energy Syst. 43 (2012) 222–229.
[11] A. Mansoor, Lower order harmonic cancellation: impact of low-voltage network topology, in: Power Engineering Society 1999 Winter Meeting, vol. 2, IEEE, 1999, pp. 1106–1109.

[12] A. Mau Teng, V.M. Jovica, Planning approaches for the strategic placement of passive harmonic filters in radial distribution networks, IEEE Trans. Power Deliv. 22 (2007) 347–353.
[13] W. Fei, J.L. Duarte, M.A.M. Hendrix, P.F. Ribeiro, Modeling and analysis of grid harmonic distortion impact of aggregated DG inverters, IEEE Trans. Power Electron 26 (2011) 786–797.
[14] J.H.R. Enslin, P.J.M. Heskes, Harmonic interaction between a large number of distributed power inverters and the distribution network, IEEE Trans. Power Electron. 19 (2004) 1586–1593.
[15] IEEE Recommended Practices and Requirements for Harmonic Control in Electrical Power Systems. IEEE Std 519-1992. 1993:0_1.
[16] F.C. De La Rosa, Harmonics and Power Systems, CRC Press Inc., Boca Raton, FL, USA, 2006.
[17] P.S. Moses, M.A.S. Masoum, Three-phase asymmetric transformer aging considering voltage–current harmonic interactions, unbalanced nonlinear loading, magnetic couplings, and hysteresis, IEEE Trans. Energy Convers. 27 (2012) 318–327.
[18] M.A.S. Masoum, P.S. Moses, Impact of balanced and unbalanced direct current bias on harmonic distortion generated by asymmetric three-phase three-leg transformers, Electr. Power Appl. IET 4 (2010) 507–515.
[19] A. Ghosh, A. Joshi, The use of instantaneous symmetrical components for balancing a delta connected load and power factor correction, Electr. Power Syst. Res. 54 (2000) 67–74.
[20] S.M. Halpin, Comparison of IEEE and IEC harmonic standards, in: Power Engineering Society General Meeting, 2005, vol. 3, IEEE, 2005, pp. 2214–2216.
[21] Staff BSI, Guide for the Application of the European Standard En 50160: BSI Standards, 2004.
[22] Commission IE, IEC 61000-3-6: Electromagnetic Compatibility (EMC) – Limits – Assessment of Emission Limits for Distorting Loads in MV and HV Power Systems – Basic, EMC Publication, Geneva, Switzerland, 1996.
[23] L. Cividino, Power factor, harmonic distortion; causes, effects and considerations, in: Telecommunications Energy Conference, 1992 INTELEC 92, 14th International, 1992, pp. 506–513.
[24] R. Arghandeh, A. Onen, J. Jung, R.P. Broadwater, Harmonic interactions of multiple distributed energy resources in power distribution networks, Electr. Power Syst. Res. 105 (2013) 124–133.
[25] J. Hambrick, R. Broadwater, Advantages of Integrated System Model-Based Control for Electrical Distribution System Automation, World Congress, Milano, Italy, 2011, pp. 6117–6120.
[26] D. Cheng, D. Zhu, R.P. Broadwater, S. Lee, A graph trace based reliability analysis of electric power systems with time-varying loads and dependent failures, Electr. Power Syst. Res. 79 (2009) 1321–1328.
[27] J. Hambrick, R.P. Broadwater, Configurable, hierarchical, model-based control of electrical distribution circuits, IEEE Trans. Power Syst. 26 (2011) 1072–1079.
[28] A. Onen, D. Cheng, R. Arghandeh, J. Jung, J. Woyak, M. Dilek, et al., Smart model based coordinated control based on feeder losses, energy consumption, and voltage violations, Electr. Power Compon. Syst. 41 (2013) 1686–1696.
[29] M. Dilek, F. de León, R. Broadwater, S. Lee, A robust multiphase power flow for general distribution networks, IEEE Trans. Power Syst. 25 (2010) 760–768.
[30] R. Arghandeh, A. Onen, J. Jung, D. Cheng, R. Broadwater, V. Centeno, Harmonic Impact Study For Distributed Energy Resources Integrated into Power Distribution Networks, in: American Society of Mechanical Engineers Power Conference 2013, (ASME Power2013), American Society of Mechanical Engineers, Boston, MA, USA, 2013, p. 8.
[31] M. Dilek, R. Broadwater, R. Sequin, Computing distribution system fault currents and voltages via numerically computed Thevenin equivalents and sensitivity matrices, in: Power Systems Conference and Exposition, 2004 IEEE PES: IEEE, 2004, pp. 244–251.
[32] W.H. Kersting, Distribution System Modeling and Analysis, CRC Press, Boca Raton, FL, USA, 2012.
[33] M. Dilek, R.P. Broadwater, J.C. Thompson, R. Seqiun, Simultaneous phase balancing at substations and switches with time-varying load patterns, IEEE Trans. Power Syst. 16 (2001) 922–928.
[34] R. Langella, A. Testa, A.E. Emanuel, Unbalance definition for electrical power systems in the presence of harmonics and interharmonics, IEEE Trans. Instrum. Meas. 61 (2012) 2622–2631.